Bioelectromagnetics 33:257–264 (2012)

Nanosecond Electric Pulses Cause Mitochondrial Membrane Permeabilization in Jurkat Cells

Tina Batista Napotnik,[1] Yu-Hsuan Wu,[2] Martin A. Gundersen,[3] Damijan Miklavčič,[1] and P. Thomas Vernier[3]*

[1]*Faculty of Electrical Engineering, University of Ljubljana, Ljubljana, Slovenija*
[2]*Mork Family Department of Materials Science and Chemical Engineering,Viterbi School of Engineering (VSoE), University of Southern California (USC), Los Angeles, California*
[3]*Ming Hsieh Department of Electrical Engineering,VSoE, USC, Los Angeles, California*

Nanosecond, high-voltage electric pulses (nsEP) induce permeabilization of the plasma membrane and the membranes of cell organelles, leading to various responses in cells including cytochrome *c* release from mitochondria and caspase activation associated with apoptosis. We report here evidence for nsEP-induced permeabilization of mitochondrial membranes in living cells. Using three different methods with fluorescence indicators—rhodamine 123 (R123), tetramethyl rhodamine ethyl ester (TMRE), and cobalt-quenched calcein—we have shown that multiple nsEP (five pulses or more, 4 ns duration, 10 MV/m, 1 kHz repetition rate) cause an increase of the inner mitochondrial membrane permeability and an associated loss of mitochondrial membrane potential. These effects could be a consequence of nsEP permeabilization of the inner mitochondrial membrane or the activation of mitochondrial membrane permeability transition pores. Plasma membrane permeabilization (YO-PRO-1 influx) was detected in addition to mitochondrial membrane permeabilization. Bioelectromagnetics 33:257–264, 2012.

Key words: mitochondrial membrane potential; permeabilization; plasma membrane; nanosecond electric pulse

INTRODUCTION

Nanosecond, high-voltage electric pulses (nsEP) with durations of up to 100 ns and electric field strengths over 1 MV/m permeabilize not only the plasma membrane [Vernier et al., 2006], but also organelles in the cell interior [Schoenbach et al., 2001; Napotnik et al., 2010]. Effects of nsEP include calcium ion release [Vernier et al., 2003b; Buescher et al., 2004], permeabilization of intracellular granules [Schoenbach et al., 2001], large endocytosed vacuoles [Tekle et al., 2005], externalization of phosphatidylserine [Vernier et al., 2004], damage of cell nuclei and DNA [Stacey et al., 2003; Vernier et al., 2005], and platelet activation [Zhang et al., 2008]. They can also provoke apoptosis [Beebe et al., 2002; Vernier et al., 2003a] and are under active investigation as a promising new tool for cancer therapy [Garon et al., 2007; Chen et al., 2009; Nuccitelli et al., 2010].

Mitochondria play a crucial role in apoptosis [Kroemer et al., 2007]. Mitochondria release several apoptosis-inducing proteins into the cytoplasm, including cytochrome *c* [Liu et al., 1996], second mitochondria-derived activator of caspase/direct IAP-binding protein with low pI (Smac/Diablo) [Du et al., 2000], AIF (apoptosis-inducing factor) [Susin et al., 1999], mitochondrial serine protease high temperature requirement protein A2 (HtrA2/Omi) [Hegde et al., 2002], and endonuclease G [Li et al., 2001]. These proteins are released from the mitochondrial intermembrane space through channels in the outer mitochondrial membrane under the control of B-cell lymphoma 2 (Bcl-2)-related proteins

Grant sponsors: Slovenian Research Agency (ARRS) (BI-US/08-10-009, Z2-7046, P2-0249); Air Force Office of Scientific Research.

Tina Batista Napotnik and Yu-Hsuan Wu contributed equally to this work.

*Correspondence to: P. Thomas Vernier, Ming Hsieh Department of Electrical Engineering, VSoE, USC, Los Angeles, CA 90067. E-mail: vernier@usc.edu

Received for review 7 April 2011; Accepted 1 September 2011

DOI 10.1002/bem.20707
Published online 23 September 2011 in Wiley Online Library (wileyonlinelibrary.com).

and/or rupture of the outer mitochondrial membrane, following the mitochondrial permeability transition [Petit et al., 1998; Kroemer et al., 2007]. Different cell types respond to apoptotic stimuli in different ways, following different pathways to apoptotic cell death [Kroemer et al., 2007]. Release of cytochrome *c* from mitochondria after applying nsEP to cells has been reported [Beebe et al., 2003; Hall et al., 2007a], and mitochondrial membrane potential was decreased in a portion of cells after exposure to 300 ns pulses [Ren and Beebe, 2011], even in the absence of cytochrome *c* release [Ford et al., 2010].

Theoretical studies predict that mitochondria could be the target of nsEP electroporation [Kotnik and Miklavcic, 2006]. AIFs could be released into the cytoplasm through nsEP-induced permeabilization of mitochondrial membranes. Therefore, we investigated the effects of nsEP (4 ns, 10 MV/m) on mitochondrial membrane permeability and mitochondrial membrane potential. A decrease in mitochondrial membrane potential indicates a change in the ability of the cell to maintain proton and other ion concentration gradients across the inner mitochondrial membrane [Kroemer et al., 2007]. We monitored mitochondrial membrane potential with rhodamine 123 (R123) and tetramethyl rhodamine ethyl ester (TMRE), fluorescent lipophilic cationic dyes that accumulate in mitochondria in a potential-dependent manner [Emaus et al., 1986; Ichas et al., 1997]. We also employed a cobalt-quenched calcein method for detecting mitochondrial membrane permeabilization [Petronilli et al., 1999]. In addition, we monitored plasma membrane permeabilization by looking for influx of the fluorescent dyes YO-PRO-1 and propidium iodide (PI). Our results are consistent with pulse-induced permeabilization of mitochondrial membranes with an associated loss of mitochondrial membrane potential.

MATERIALS AND METHODS

Cell Line and Cell Culture

Human Jurkat T lymphoblasts (obtained from American Type Culture Collection (ATCC), Manassas, VA; ATCC cell number: TIB-152) were grown in RPMI-1640 medium (Mediatech, Manassas, VA) containing 10% heat-inactivated fetal bovine serum (Gibco/Invitrogen, Carlsbad, CA), 2 mM L-glutamine (Gibco/Invitrogen), 50 units/ml penicillin (Gibco/Invitrogen), and 50 μg/ml streptomycin (Gibco/Invitrogen). Cells were cultured at 37 °C in a humidified, 5% carbon dioxide atmosphere and concentrated to 2×10^7 cells/ml for pulse treatment.

Pulse Generator and Pulse Exposure

For microscopic observation, cells were placed in a microchamber 100 μm wide, 30 μm deep, and 15 mm long with platinum electrode walls, on a glass microscope slide. A resonant-charged, solid-state Marx bank-driven, hybrid-core compression, diode-opening switch pulse generator, designed and assembled at the University of Southern California (Los Angeles, CA) [Sanders et al., 2009], delivered 4 ns, 10 MV/m electrical pulses at a 1 kHz repetition rate to the microchamber electrodes mounted on the microscope stage in ambient atmosphere at room temperature. The impedance of the microchamber load, when it was loaded with a cell suspension in our standard media, was about 350 Ω.

Fluorescence Microscopy and Fluorescent Molecular Probes

Observations of live cells during pulse exposures were made using a Zeiss Axiovert 200 epifluorescence microscope (Zeiss, Göttingen, Germany) with a 63× water immersion objective and a Hamamatsu ImageEM EM-CCD camera (Hamamatsu Photonics KK, Hamamatsu City, Japan). Captured images were analyzed with Hamamatsu SimplePCI software. Cells were stained with the fluorescent probes for mitochondria (cobalt-quenched calcein, R123, TMRE, and MitoTrackers) and for plasma membrane permeability (PI and YO-PRO-1).

Cobalt-quenched calcein. Calcein-AM (Molecular Probes/Invitrogen, Carlsbad, CA) is an anionic fluorochrome that enters cells freely and labels cytoplasmic as well as mitochondrial regions following removal of the acetoxymethyl (AM) group by intracellular esterases. Because cobalt ions are taken up by cells but do not readily pass through the mitochondrial membrane, mitochondria can be identified by the cobalt quenching of cytoplasmic, but not mitochondrial, calcein fluorescence [Hüser et al., 1998; Petronilli et al., 1999]. Cells were loaded with 500 nM calcein-AM in the presence of 1 mM $CoCl_2$ at 37 °C in a 5% CO_2 atmosphere for 20 min. Before pulse treatment, cells were washed and resuspended in fresh RPMI-1640 medium with or without 1 mM Co^{2+}. Fluorescent images were captured before pulsing and 3 min after pulsing, using the appropriate filter (Ex 482/35, Em 536/40, and D 506DCLP). For quantification, the cells in the images were encircled and the fluorescence of cells was measured. The background fluorescence was subtracted. The results were expressed relative to cells before pulsing.

Mitochondrial membrane potential. Rhodamine 123 (R123) and TMRE were used to assess changes in mitochondrial membrane potential [Emaus et al., 1986; Chen, 1988; Scaduto and Grotyohann, 1999]. Cells were incubated with 1 μM R123 (Molecular Probes/Invitrogen) for 45 min, or 50 nM TMRE (Molecular Probes/Invitrogen) for 20 min. After incubation, cells were centrifuged and resuspended in fresh RPMI-1640 medium for pulse exposure. Fluorescent images were captured before pulsing and 30 s and 3 min after pulsing, using the appropriate filters (R123: Ex 482/35, Em 536/40, D 506DCLP; TMRE: Ex 543/22, Em 593/40, D 562DCLP). For quantification, the cells in the images were encircled and the fluorescence of cells was measured. The background fluorescence was subtracted. The results were expressed relative to cells before pulsing.

For a positive control, the proton ionophore uncoupler of oxidative respiration carbonyl cyanide 3-chlorophenylhydrazone (CCCP) was added to the R123- or TMRE-stained cells in suspension at 20 μM [Bortner and Cidlowski, 1999]. Images were captured and quantified the same way as pulsed cells, only the results were expressed relative to cells that were not treated with CCCP.

MitoTrackers. MitoTracker Green and MitoTracker Orange (Molecular Probes/Invitrogen) were used to confirm the labeling of mitochondria by double labeling (MitoTracker Orange with cobalt-quenched calcein and R123, and MitoTracker Green with TMRE). Cell loading was performed according to the manufacturer's protocol (100 nM MitoTracker Orange and 50 nM MitoTracker Green). Images of double-stained cells were captured by using appropriate filters (MitoTracker Orange: Ex 543/22, Em 593/40, D 562DCLP; MitoTracker Green: Ex 482/35, Em 536/40, D 506DCLP).

Plasma membrane permeability. Intracellular YO-PRO-1 (Molecular Probes/Invitrogen) and PI (Molecular Probes/Invitrogen) fluorescence were used as indicators of plasma membrane permeabilization as described previously [Vernier et al., 2006]. Cells were suspended in RPMI-1640 medium with 10 μM YO-PRO-1 or 7.5 μM PI just before pulsing. Fluorescent images were captured before pulsing and 3 min after pulsing, using the appropriate filters (YO-PRO-1: Ex 472/30, Em 520/35, D 495DCLP; PI: Ex 562/40, Em 624/40, D 593DCLP). For quantification, cells in the images were encircled and the fluorescence of cells was measured. The background fluorescence was subtracted. The results were expressed in arbitrary units.

RESULTS

Localization of Mitochondria

Jurkat T lymphoblasts were stained with three fluorescent labeling methods specific for mitochondria: cobalt-quenched calcein, rhodamine 123 (R123), and TMRE. Mitochondria in cells are seen as bright spots in the cytoplasm. Co-labeling with MitoTracker Orange or MitoTracker Green revealed almost complete overlap of the MitoTracker dyes with the structures stained with R123 and TMRE (Fig. 1). The bright particles in calcein-stained cells are not dense enough to merge over the entire intracellular area labeled by the MitoTracker dyes, but the calcein-labeled regions are coincident with the MitoTracker-labeled regions.

nsEP Pulses Cause a Loss of Mitochondrial Potential in Jurkat Cells

R123 and TMRE are lipophilic cationic dyes that accumulate in active mitochondria because of the large negative potential that appears across normal mitochondrial membranes. When the mitochondrial membrane potential decreases, the concentration of these dyes in the mitochondria decreases with an associated decrease in R123 and TMRE fluorescence. Our results show that nsEPs cause a significantly reduced fluorescence of both dyes, indicating a loss of mitochondrial membrane potential (Figs. 2 and 3). The extent of pulse-induced mitochondrial membrane permeabilization depends on the number of pulses—more pulses cause a greater reduction in R123 and TMRE fluorescence. At 10 pulses (4 ns, 10 MV/m, 1 kHz repetition frequency), R123 and TMRE fluorescence decreased to 76% and 78% of pre-pulse fluorescence, respectively. At 50 pulses, R123 and TMRE fluorescence decreased to 63% and 30% of the pre-pulse fluorescence emission, respectively. CCCP, a proton ionophore uncoupler that causes a loss of mitochondrial membrane potential [Bortner and Cidlowski, 1999], was used as a positive control. After exposing the cells to CCCP (Figs. 2 and 3) fluorescence decreased to 61% and 12% of control cells for R123 and TMRE, respectively.

Plasma Membrane Permeabilization After nsEP Application

We labeled mitochondria with cobalt-quenched calcein and suspended cells in the medium without

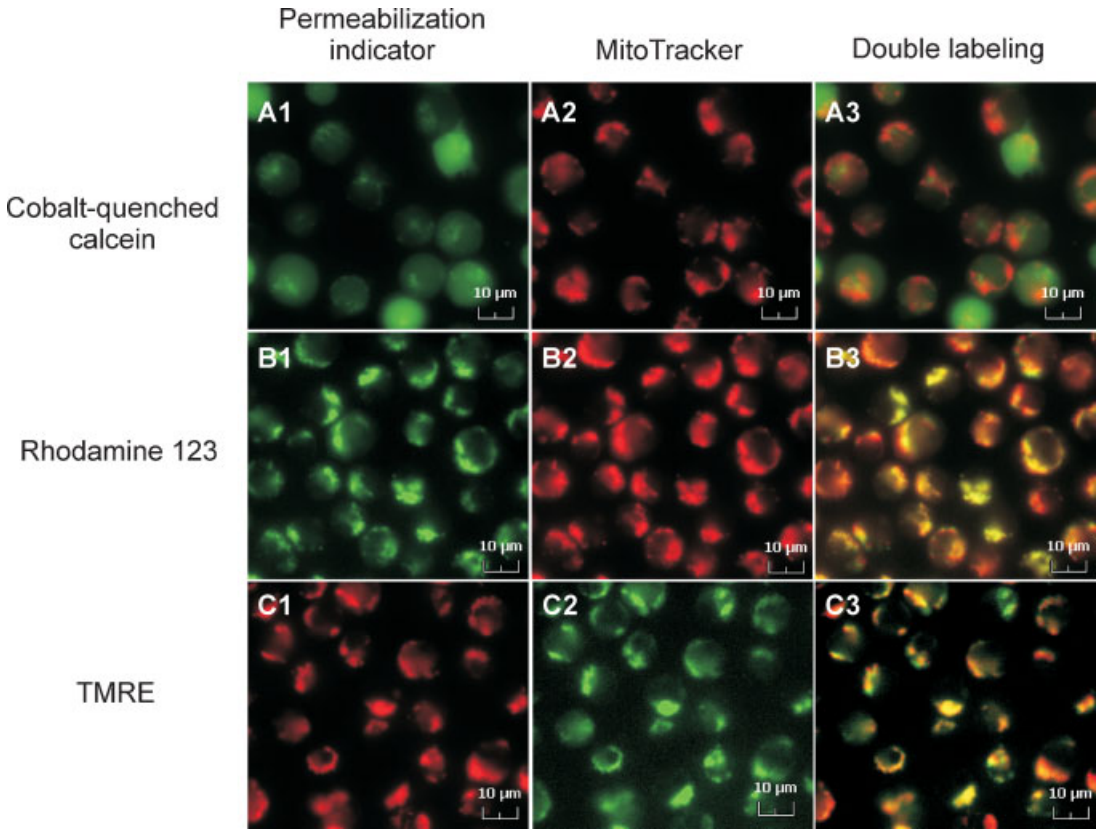

Fig. 1. Localization of mitochondria in Jurkat cells. Cells were loaded with cobalt-quenched calcein (**A**), R123 (**B**), or TMRE (**C**), with MitoTracker Orange (A,B) or MitoTracker Green (C). **A1**–**C1**: permeabilization indicator images. **A2**–**C2**: MitoTracker images. **A3**–**C3**: superimposed images.

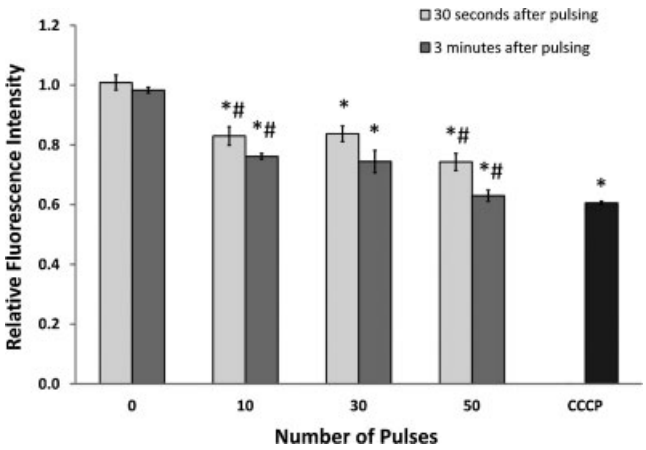

Fig. 2. Dose-dependent R123 fluorescence intensity before and after pulsing (mean ± SEM). CCCP was used as positive control. Significant differences from zero-pulse controls are designated by asterisks ($^{*}P < 0.05$). $^{\#}$Statistically different from previous column of same incubation time ($P < 0.05$). There are at least 60 cells for each data point and each condition was repeated at least three times.

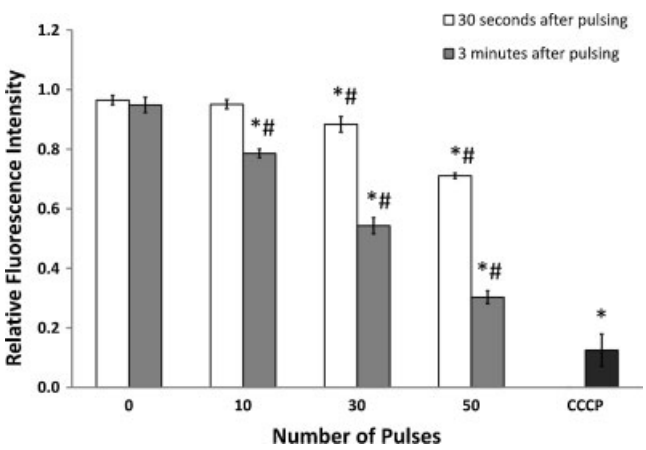

Fig. 3. Dose-dependent TMRE fluorescence intensity before and after pulsing (mean ± SEM). CCCP was used as positive control. Significant differences from zero-pulse controls are designated by asterisks ($^{*}P < 0.05$). $^{\#}$Statistically different from previous column of same incubation time ($P < 0.05$). There are at least 124 cells for each data point and each condition was repeated at least three times.

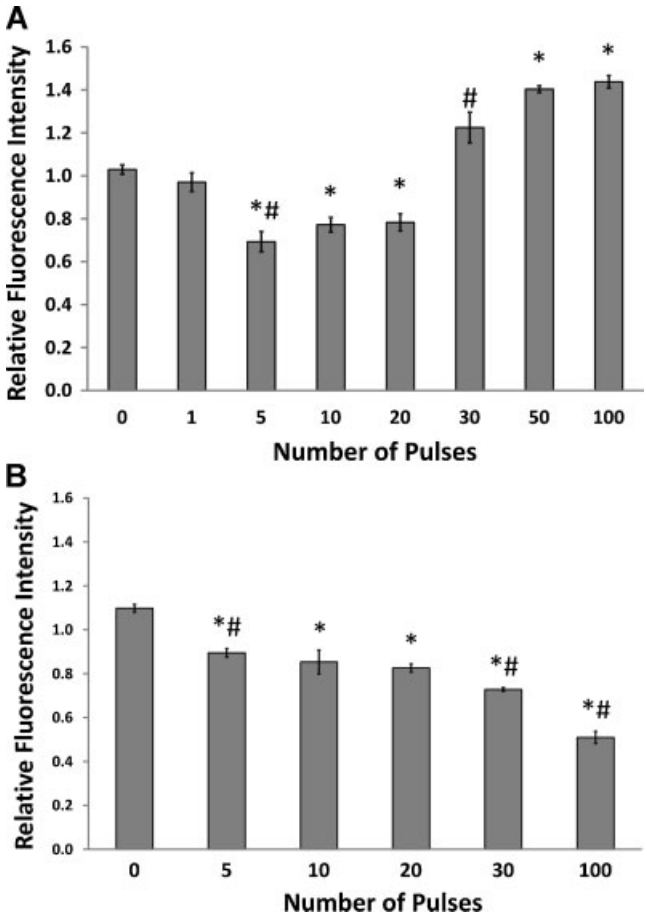

Fig. 4. Dose-dependent calcein fluorescence without (**A**) or with (**B**) Co^{2+} in the medium. Data show the relative fluorescence intensity before and 3 min after pulsing (mean ± SEM). Significant differences from zero-pulse controls are designated by asterisks ($^{*}P < 0.05$). $^{\#}$Statistically different from previous column ($P < 0.05$). There are at least 38 cells for each data point and each condition was repeated at least three times.

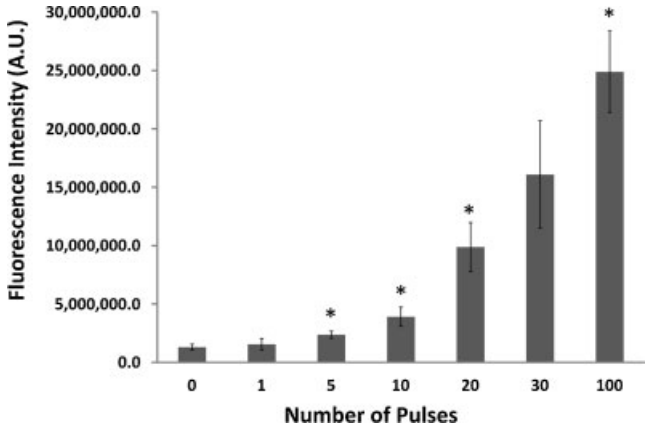

Fig. 5. Dose-dependent YO-PRO-1 uptake. Fluorescence images were recorded 3 min after pulse exposure. Data show YO-PRO-1 fluorescence 3 min after pulsing (mean ± SEM) in arbitrary units. Significant differences from zero-pulse controls are designated by asterisks ($^{*}P < 0.05$). There are at least 36 cells for each data point and each condition was repeated at least three times.

or with cobalt ions. When calcein-stained, cobalt-quenched cells were exposed to nsEP in the medium without cobalt ions in the external medium (Fig. 4A), calcein fluorescence emission decreased after exposure to 5, 10, and 20 pulses, indicating mitochondrial membrane permeabilization. No fluorescence decrease was observed after exposure to 30 pulses or more under these conditions, suggesting that plasma membrane permeabilization at these higher pulse numbers allows cobalt ions to leak out of the cells, dequenching the calcein fluorescence; hence, the fluorescence emission of calcein in cells was high.

On the other hand, when calcein-stained, cobalt-quenched cells were treated in medium with cobalt ions (Fig. 4B), the calcein fluorescence decreased significantly after the application of 5 nsEP pulses and decreased further at higher pulse numbers (30–100). The extent of mitochondrial permeabilization depends on the number of pulses applied since the fluorescence is lower with higher pulse numbers; it decreased to 73% and 51% of the fluorescence before pulsing with 30 and 100 pulses, respectively. These results suggest that cobalt ions in the external medium allow sufficient calcein quenching even after permeabilization of the plasma membrane since the Co^{2+} concentration gradient favors an inward flux of cobalt ions rather than a decrease in cytoplasmic Co^{2+}.

In addition, plasma membrane permeabilization was monitored with YO-PRO-1 and PI uptake. YO-PRO-1 influx is significantly increased at five or more pulses (Fig. 5). Fluorescence intensity increased 8, 12, and 19 times higher than in untreated control cells after applying 20, 30, and 100 pulses, respectively. Although PI is a less sensitive detector of plasma membrane permeabilization than YO-PRO-1 [Vernier et al., 2006], a measurable influx of PI was detected after applying 20 pulses or more (Fig. 6). PI fluorescence intensity increased three and four times higher than in untreated control cells after applying 20 and 30 pulses, respectively.

DISCUSSION

Using three different indicators of mitochondrial membrane integrity in living cells, we have shown that high-voltage, nanosecond electric pulses (4 ns, 10 MV/m, 1 kHz repetition rate) cause an increase in mitochondrial membrane permeability and an associated decrease in mitochondrial membrane potential. In addition, we have observed that with these pulse

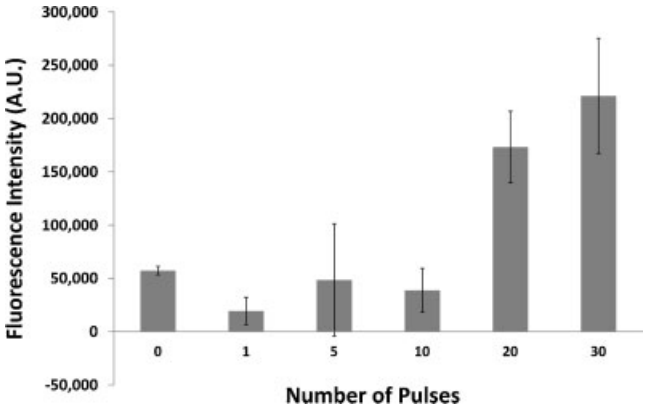

Fig. 6. Dose-dependent propidium uptake. Fluorescence images were recorded 3 min after pulse exposure. Data show PI fluorescence 3 min after pulsing (mean ± SEM) in arbitrary units. There are at least 32 cells for each data point and each condition was repeated at least three times.

parameters, exposure to fewer pulses ($<$20) permeabilize the mitochondrial membrane while leaving the plasma membrane relatively impermeable to propidium yet permeable to small but significant amounts of YO-PRO-1 (after five pulses, fluorescence reached 1.8 times the value of control cells). Higher pulse numbers ($\geq$20), however, produce significant plasma and mitochondrial membrane permeabilization. These relative permeabilization sensitivities are consistent with our observations of intracellular cobalt-quenched calcein fluorescence with and without cobalt in the external medium.

Exposure of cells to nsEP provokes apoptosis in vitro [Beebe et al., 2002] and in mice [Beebe et al., 2002; Nuccitelli et al., 2009], but the mechanisms for nsEP induction of apoptosis have not been established. Mitochondria play a crucial role in apoptosis, and disruption of the normal barrier functions of the mitochondrial membranes is a key step in this process during which mitochondria release several apoptosis-inducing proteins, especially from the intermembrane mitochondrial space into the cytoplasm where they further activate the execution of apoptosis [reviewed in Wang, 2001; Kroemer et al., 2007]. Cytochrome *c* is released through pores in the outer mitochondrial membrane that are formed by pro-apoptotic molecules such as Bcl-2-associated X protein (BAX) and Blc-2 homologous antagonist/killer (BAK) [Ow et al., 2008], or by the opening of the outer mitochondrial membrane that occurs after the mitochondrial permeability transition [Hunter et al., 1976; Danial and Korsmeyer, 2004; Bernardi et al., 2006; Kroemer et al., 2007]. It is already known that mitochondria release cytochrome *c* after nsEP exposure [Beebe et al., 2003; Hall et al., 2007b], but it has not been established whether this is a consequence of Bcl-2-family-induced permeabilization of the outer mitochondrial membrane or a direct consequence of nsEP poration of mitochondrial membranes.

In our present work we observe nsEP-induced decreases in the fluorescence emissions of R123, TMRE, and cobalt-quenched calcein, consistent with the hypothesis that nsEP exposure permeabilizes the inner membrane of mitochondria with an associated loss in the mitochondrial membrane potential. A significant decrease in the mitochondrial membrane potential was observed after applying 5–30 pulses (4 ns, 10 MV/m, 1 kHz repetition rate), depending on the sensitivities of the detection methods. Measuring R123 and TMRE fluorescence emissions at different time points (30 s and 3 min) showed that this is a progressive event, lasting at least several minutes after pulsing. TMRE, a dye which shows less binding than R123 and is also rapidly and reversibly taken up by live cells and therefore more suitable for dynamic measurements [Ehrenberg et al., 1988; Loew et al., 1993], exhibited a more rapid decrease in fluorescence emission compared to R123. Theoretical studies predict that mitochondria could be the target of nsEP electroporation [Kotnik and Miklavcic, 2006], and it has been shown that nsEP exposure causes permeabilization of intracellular organelles such as intracellular granules of granulocytes [Schoenbach et al., 2001], large endocytosed vacuoles [Tekle et al., 2005], and endocytotic vesicles [Rebersek et al., 2009; Napotnik et al., 2010]. However, we cannot conclude with certainty from the results reported here whether the nsEP-induced decrease in the mitochondrial membrane potential results from the direct electroporation of the inner mitochondrial membrane or the formation of mitochondrial membrane permeability transition pores, or from some other permeabilizing mechanism. Since nsEP also causes plasma membrane permeabilization (as observed by cobalt-quenched calcein and YO-PRO-1 and PI influx) other molecules and ions including calcium ions could enter the cell and trigger the mitochondrial permeability transition [Lemasters et al., 2009] as a secondary effect of plasma membrane permeabilization.

We interpret the combination of the cobalt-quenched calcein and YO-PRO-1 and PI influx results to mean that significant plasma membrane permeabilization occurs with pulse numbers $>$20. This apparent threshold is at least in part a consequence of the detection sensitivity of the methods. We already know that YO-PRO-1 is a more sensitive indicator of plasma membrane permeabilization than

PI [Vernier et al., 2006; Bowman et al., 2010], and we see evidence of PI influx with a 20-pulse exposure under the conditions we employed in this work, while at the same time even 5 pulses results in measurable YO-PRO-1 entry into the cell. Similarly, and perhaps not coincidentally, we observed an increase in calcein fluorescense with a pulse number above 20 using the cobalt-quenched calcein method for mitochondrial labeling without Co^{2+} in the medium, suggesting a leak of intracellular Co^{2+} through the permeabilized plasma membrane, resulting in calcein dequenching. This interpretation is supported by the observation that no dequenching is observed when Co^{2+} is present in the suspending medium at the loading (quenching) concentration. It should be emphasized that the cobalt-quenched calcein method for highlighting mitochondria, like the other methods, is used here as a qualitative indicator of intracellular pulse effects and not as a basis for quantitative conclusions.

We also note that Ren and Beebe [2011] showed that with longer, 300 ns pulses (10 pulses, 6 MV/m) the mitochondrial membrane potential decreased in about 50% of cells (15 min after pulsing), whereas PI uptake occurred in more than 95% of cells, suggesting that 300 ns pulses are not short enough to efficiently induce intracellular effects. With much shorter, 4 ns pulses we observe more pronounced intracellular membrane permeabilization and less permeabilization of the plasma membrane.

In conclusion, using three different methods with fluorescence indicators—rhodamine 123, TMRE, and cobalt-quenched calcein—we show that nsEP (4 ns duration, 10 MV/m, 1 kHz repetition rate) cause a loss of the mitochondrial membrane potential. The most likely explanation for this observation is nsEP permeabilization of the inner mitochondrial membrane, although it is possible that nsEP exposure triggers the mitochondrial permeability transition through some mechanism still to be identified. At the same time, we also detected plasma membrane permeabilization, indicated by YO-PRO-1 influx and the responses of cobalt-quenched calcein-labeled cells.

ACKNOWLEDGMENTS

We gratefully thank Jason Sanders for pulse generator engineering expertise.

REFERENCES

Beebe SJ, Fox PM, Rec LJ, Somers K, Stark RH, Schoenbach KH. 2002. Nanosecond pulsed electric field (nsPEF) effects on cells and tissues: Apoptosis induction and tumor growth inhibition. IEEE Trans Plasma Sci 30(1):286–292.

Beebe SJ, Fox PM, Rec LJ, Willis EL, Schoenbach KH. 2003. Nanosecond, high-intensity pulsed electric fields induce apoptosis in human cells. FASEB J 17(11):1493–1495.

Bernardi P, Krauskopf A, Basso E, Petronilli V, Blachly-Dyson E, Blalchy-Dyson E, Di Lisa F, Forte M. 2006. The mitochondrial permeability transition from in vitro artifact to disease target. FEBS J 273(10):2077–2099.

Bortner CD, Cidlowski JA. 1999. Caspase independent/dependent regulation of K(+), cell shrinkage, and mitochondrial membrane potential during lymphocyte apoptosis. J Biol Chem 274(31):21953–21962.

Bowman AM, Nesin OM, Pakhomova ON, Pakhomov AG. 2010. Analysis of plasma membrane integrity by fluorescent detection of Tl(+) uptake. J Membr Biol 236(1):15–26.

Buescher ES, Smith RR, Schoenbach K. 2004. Submicrosecond intense pulsed electric field effects on intracellular free calcium: Mechanisms and effects. IEEE Trans Plasma Sci 32(4):1563–1572.

Chen LB. 1988. Mitochondrial membrane potential in living cells. Annu Rev Cell Biol 4:155–181.

Chen XH, Swanson RJ, Kolb JF, Nuccitelli R, Schoenbach KH. 2009. Histopathology of normal skin and melanomas after nanosecond pulsed electric field treatment. Melanoma Res 19(6):361–371.

Danial N, Korsmeyer S. 2004. Cell death: Critical control points. Cell 116(2):205–219.

Du C, Fang M, Li Y, Li L, Wang X. 2000. Smac, a mitochondrial protein that promotes cytochrome c-dependent caspase activation by eliminating IAP inhibition. Cell 102(1):33–42.

Ehrenberg B, Montana V, Wei MD, Wuskell JP, Loew LM. 1988. Membrane potential can be determined in individual cells from the Nernstian distribution of cationic dyes. Biophys J 53(5):785–794.

Emaus R, Grunwald R, Lemasters J. 1986. Rhodamine 123 as a probe of transmembrane potential in isolated rat-liver mitochondria: Spectral and metabolic properties. Biochim Biophys Acta 850(3):436–448.

Ford WE, Ren W, Blackmore PF, Schoenbach KH, Beebe SJ. 2010. Nanosecond pulsed electric fields stimulate apoptosis without release of pro-apoptotic factors from mitochondria in B16f10 melanoma. Arch Biochem Biophys 497(1–2):82–89.

Garon EB, Sawcer D, Vernier PT, Tang T, Sun YH, Marcu L, Gundersen MA, Koeffler HP. 2007. In vitro and in vivo evaluation and a case report of intense nanosecond pulsed electric field as a local therapy for human malignancies. Int J Cancer 121(3):675–682.

Hall E, Schoenbach K, Beebe S. 2007a. Nanosecond pulsed electric fields induce apoptosis in p53-wildtype and p53-null HCT116 colon carcinoma cells. Apoptosis 12(9):1721–1731.

Hall EH, Schoenbach KH, Beebe SJ. 2007b. Nanosecond pulsed electric fields have differential effects on cells in the S-phase. DNA Cell Biol 26(3):160–171.

Hegde R, Srinivasula S, Zhang Z, Wassell R, Mukattash R, Cilenti L, DuBois G, Lazebnik Y, Zervos A, Fernandes-Alnemri T, Alnemri ES. 2002. Identification of Omi/HtrA2 as a mitochondrial apoptotic serine protease that disrupts inhibitor of apoptosis protein-caspase interaction. J Biol Chem 277(1):432–438.

Hunter D, Haworth R, Southard J. 1976. Relationship between configuration, function, and permeability in calcium-treated mitochondria. J Biol Chem 251(16):5069–5077.

Hüser J, Rechenmacher CE, Blatter LA. 1998. Imaging the permeability pore transition in single mitochondria. Biophys J 74(4):2129–2137.

Ichas F, Jouaville L, Mazat J. 1997. Mitochondria are excitable organelles capable of generating and conveying electrical and calcium signals. Cell 89(7):1145–1153.

Kotnik T, Miklavcic D. 2006. Theoretical evaluation of voltage inducement on internal membranes of biological cells exposed to electric fields. Biophys J 90(2):480–491.

Kroemer G, Galluzzi L, Brenner C. 2007. Mitochondrial membrane permeabilization in cell death. Physiol Rev 87(1):99–163.

Lemasters JJ, Theruvath TP, Zhong Z, Nieminen AL. 2009. Mitochondrial calcium and the permeability transition in cell death. Biochim Biophys Acta 1787(11):1395–1401.

Li L, Luo X, Wang X. 2001. Endonuclease G is an apoptotic DNase when released from mitochondria. Nature 412(6842):95–99.

Liu X, Kim C, Yang J, Jemmerson R, Wang X. 1996. Induction of apoptotic program in cell-free extracts: Requirement for dATP and cytochrome c. Cell 86(1):147–157.

Loew LM, Tuft RA, Carrington W, Fay FS. 1993. Imaging in five dimensions: Time-dependent membrane potentials in individual mitochondria. Biophys J 65(6):2396–2407.

Napotnik T, Rebersek M, Kotnik T, Lebrasseur E, Cabodevila G, Miklavcic D. 2010. Electropermeabilization of endocytotic vesicles in B16 F1 mouse melanoma cells. Med Biol Eng Comput 48(5):407–413.

Nuccitelli R, Chen X, Pakhomov AG, Baldwin WH, Sheikh S, Pomicter JL, Ren W, Osgood C, Swanson RJ, Kolb JF, Beebe SJ, Schoenbach KH. 2009. A new pulsed electric field therapy for melanoma disrupts the tumor's blood supply and causes complete remission without recurrence. Int J Cancer 125(2):438–445.

Nuccitelli R, Tran K, Sheikh S, Athos B, Kreis M, Nuccitelli P. 2010. Optimized nanosecond pulsed electric field therapy can cause murine malignant melanomas to self-destruct with a single treatment. Int J Cancer 127(7): 1727–1736.

Ow Y, Green D, Hao Z, Mak T. 2008. Cytochrome c: Functions beyond respiration. Nat Rev Mol Cell Biol 9(7):532–542.

Petit P, Goubern M, Diolez P, Susin S, Zamzami N, Kroemer G. 1998. Disruption of the outer mitochondrial membrane as a result of large amplitude swelling: The impact of irreversible permeability transition. FEBS Lett 426(1): 111–116.

Petronilli V, Miotto G, Canton M, Brini M, Colonna R, Bernardi P, Di Lisa F. 1999. Transient and long-lasting openings of the mitochondrial permeability transition pore can be monitored directly in intact cells by changes in mitochondrial calcein fluorescence. Biophys J 76(2):725–734.

Rebersek M, Kranjc M, Pavliha D, Batista-Napotnik T, Vrtacnik D, Amon S, Miklavcic D. 2009. Blumlein configuration for high-repetition-rate pulse generation of variable duration and polarity using synchronized switch control. IEEE Trans Biomed Eng 56(11):2642–2648.

Ren W, Beebe SJ. 2011. An apoptosis targeted stimulus with nanosecond pulsed electric fields (nsPEFs) in E4 squamous cell carcinoma. Apoptosis 16(4):382–393.

Sanders J, Kuthi A, Wu Y, Vernier P, Gundersen M. 2009. A linear, single-stage, nanosecond pulse generator for delivering intense electric fields to biological loads. IEEE Trans Dielect Elec Ins 16(4):1048–1054.

Scaduto RC, Grotyohann LW. 1999. Measurement of mitochondrial membrane potential using fluorescent rhodamine derivatives. Biophys J 76(1 Pt 1):469–477.

Schoenbach KH, Beebe SJ, Buescher ES. 2001. Intracellular effect of ultrashort electrical pulses. Bioelectromagnetics 22(6):440–448.

Stacey M, Stickley J, Fox P, Statler V, Schoenbach K, Beebe SJ, Buescher S. 2003. Differential effects in cells exposed to ultra-short, high intensity electric fields: Cell survival, DNA damage, and cell cycle analysis. Mutat Res 542(1–2):65–75.

Susin S, Lorenzo H, Zamzami N, Marzo I, Snow B, Brothers G, Mangion J, Jacotot E, Costantini P, Loeffler M, Larochette N, Goodlett DR, Aebersold R, Siderovski DP, Penninger JM, Kroemer G. 1999. Molecular characterization of mitochondrial apoptosis-inducing factor. Nature 397(6718): 441–446.

Tekle E, Oubrahim H, Dzekunov SM, Kolb JF, Schoenbach KH, Chock PB. 2005. Selective field effects on intracellular vacuoles and vesicle membranes with nanosecond electric pulses. Biophys J 89(1):274–284.

Vernier PT, Li AM, Marcu L, Craft CM, Gundersen MA. 2003a. Ultrashort pulsed electric fields induce membrane phospholipid translocation and caspase activation: Differential sensitivities of Jurkat T lymphoblasts and rat glioma C6cells. IEEE Trans Dielect Elec Ins 10(5):795–809.

Vernier PT, Sun YH, Marcu L, Salemi S, Craft CM, Gundersen MA. 2003b. Calcium bursts induced by nanosecond electric pulses. Biochem Biophys Res Commun 310(2):286–295.

Vernier PT, Sun YH, Marcu L, Craft CM, Gundersen MA. 2004. Nanoelectropulse-induced phosphatidylserine translocation. Biophys J 86(6):4040–4048.

Vernier PT, Sun Y, Wang J, Thu MM, Garon E, Valderrabano M, Marcu L, Koeffler HP, Gundersen MA. 2005. Nanoelectropulse intracellular perturbation and electropermeabilization technology: Phospholipid translocation, calcium bursts, chromatin rearrangement, cardiomyocyte activation, and tumor cell sensitivity. Conf Proc IEEE Eng Med Biol Soc 6:5850–5853.

Vernier PT, Sun YH, Gundersen MA. 2006. Nanoelectropulse-driven membrane perturbation and small molecule permeabilization. BMC Cell Biol 7:16.

Wang X. 2001. The expanding role of mitochondria in apoptosis. Genes Dev 15(22):2922–2933.

Zhang J, Blackmore P, Hargrave B, Xiao S, Beebe S, Schoenbach K. 2008. Nanosecond pulse electric field (nanopulse): A novel non-ligand agonist for platelet activation. Arch Biochem Biophys 471(2):240–248.